CD13 in cell adhesion: aminopeptidase N (CD13) mediates homotypic aggregation of monocytic cells

Paola Mina-Osorio,* Linda H. Shapiro,† and Enrique Ortega*,[1]

Department of Immunology, Instituto de Investigaciones Biomédicas, Universidad Nacional Autónoma de México, México D.F.; and †Department of Cellular Biology, Center for Vascular Biology, University of Connecticut Health Center, Farmington

Abstract: Homotypic aggregation (HA) of cells plays key roles in physiological and pathological processes, such as embryogenesis, immune responses, angiogenesis, tumor cell invasion, and metastasis. Aminopeptidase N (CD13) has been implicated in most of these phenomena, although its participation has been attributed to its enzymatic activity, while its role as an adhesion molecule has been almost unexplored. Here, we show that certain anti-CD13 monoclonal antibodies induce HA of monocytic U-937 cells, independently of their effect on enzymatic activity. The phenomenon is related to binding to a specific site on the CD13 molecule and is independent of integrins. It is abrogated by low temperature, by the glycolysis inhibitor 2-deoxyglucose, and by inhibitors of tyrosine and mitogen-activated protein kinases. The inhibitor of microtubule polymerization colchicine has a synergistic effect on CD13-mediated aggregation, suggesting an inhibitory role of microtubules in this process. Finally, during HA, CD13 actively redistributes to the zones of cell-cell contact, as determined by live cell imaging studies, demonstrating a direct role of CD13 in the adhesion phenomenon. Together, these data show for the first time the participation of CD13 in monocytic cell adhesion. *J. Leukoc. Biol.* 79: 719–730; 2006.

Key Words: *monocytes · laser scanning confocal microscopy · U-937*

INTRODUCTION

Aminopeptidase N (CD13) is a metalloproteinase (EC 3.4.11.2) expressed in many tissues [1, 2]. It functions as a viral receptor [3, 4] and participates in a great variety of processes, including angiogenesis [5–7], tumor cell invasion, and metastasis [8, 9]. Because of its enzymatic activity, it regulates several vasoactive peptides, neuropeptides, hormones, and cytokines [10, 11].

CD13 involvement in cell-cell interactions has not been well-studied. However, early work by Menrad et al. [12] demonstrated that CD13 is distributed homogeneously on single malignant melanoma cells but relocates to the zones of cell-cell contact in homotypic cellular aggregates and to cell substrate adhesion sites, with filopodia showing a strong CD13 signal, suggesting a role for this molecule in cellular adhesion. It is surprising that although myeloid cells express the highest levels of CD13, a possible role for CD13 in monocytic intercellular interactions has been largely unexplored. In the promonocytic cell line U-937 and in primary human monocytes and macrophages, we have reported that CD13 accumulates in zones of the membrane presenting filopodia and redistributes to the zones of contact between monocytic cells and their phagocytic targets [13]. These phenomena could be associated with a role for CD13 or its possible ligands in adhesion-related functions in myeloid cells.

Homotypic aggregation (HA) of cells plays key roles in physiological processes related to embryogenesis, angiogenesis, and immune responses, as well as in the pathogenesis of diseases such as cancer, where it contributes to neoangiogenesis, tumor cell invasion, and metastasis. For example, in immunobiology, cell-cell and cell-matrix interactions are crucial for antigen presentation, cytotoxicity, phagocytosis, leukocyte homing, and transendothelial migration [14, 15]. In tumor cell biology, during the postintravasation phases of tumor cells, HA has been proposed to play an important role in the establishment of metastasis by some types of tumors. For instance, Glinsky et al. [16] reported that heterotypic adhesion of breast and prostate metastatic cells to the endothelium and subsequent homotypic cell adhesion participate in hematogenous cancer metastasis. Finally, in angiogenesis, homotypic adhesion of endothelial cells is considered to be a crucial step in extension of new vessels [17].

Thus, as a role for CD13 has been established in several phenomena involving cell aggregation, such as tumor cell invasion, angiogenesis, and phagocytosis [9, 13], and given the importance of monocytes/macrophages in all of these processes, we evaluated a possible role of CD13 in HA between monocytic cells. In this cell type, several monoclonal antibodies (mAb) capable of inducing HA have been described using U-937 cells as a model. Among them are antibodies against CD98 [18], CD43 [19], CD147 [20], and CD29 [14, 21, 22].

[1] Correspondence: Departamento de Inmunología, Instituto de Investigaciones Biomédicas, UNAM, Circuito Escolar, S/N Ciudad Universitaria, México D.F., C.P. 04510 Mexico. E-mail: ortsoto@servidor.unam.mx

Received July 30, 2005; revised November 28, 2005; accepted November 29, 2005; doi: 10.1189/jlb.0705425.

Here, we report that mAb against CD13 induce HA of the U-937 cell line and make an initial characterization of the process.

MATERIALS AND METHODS

Cells and antibodies

The promonocytic cell line U-937 (obtained from the American Type Cell Culture Collection, Manassas, VA) was cultured in RPMI-1640 medium (Invitrogen, Grand Island, NY), supplemented with 10% heat-inactivated fetal bovine serum (FBS), 1 mM minimal essential medium (MEM) sodium pyruvate solution, 2 mM MEM nonessential amino acids solution, 0.1 mM L-glutamine, 100 U/ml penicillin, and 100 μg/ml streptomycin (Invitrogen). Cultures were maintained in a humidified atmosphere at 37°C with 6% CO_2. Murine monoclonal anti-human CD13 (Clone 452) was purified from the culture supernatant of the hybridoma, kindly donated by Dr. Meenhard Herlyn (The Wistar Institute of Anatomy and Biology, Philadelphia, PA). $F(ab)'_2$ and Fab fragments of this antibody were prepared with immobilized Ficin (Pierce, Rockford, IL). mAb labeling with Texas Red®-X succinimidyl ester (Molecular Probes, Eugene, OR) was carried out as indicated by the manufacturer. Monoclonal anti-human CD13 (Clone WM-4.7) was from Sigma Chemical Co. (St. Louis, MO). Monoclonal anti-human CD13 (Clone WM-15) was from BD PharMingen (San Diego, CA). Monoclonal anti-human CD13 (Clone MY7), CD98 (Clone 4F2), CD18 (Blocking Clone 7E4), CD11a (Blocking Clone 25.3), CD54 (Blocking Clone 84H10), CD29 (Blocking Clone 4B4), and their fluorescein isothiocyanate (FITC) conjugates were from Coulter-Immunotech (Miami, FL). Goat anti-mouse immunoglobulin (IgG) FITC was from Zymed (San Francisco, CA). Anti-Grb2 and anti-Sos polyclonal antibodies were from Santa Cruz Biotechnology (CA).

HA assays

U-937 cells (5×10^4) in 50 μl RPMI 1640, with or without anti-CD13 mAb at the indicated concentration, were placed in flat-bottom wells of a 96-well culture plate. An equal volume of medium, with or without the indicated inhibitor, was added to each well, and cells were incubated at 37°C for different periods of time (0.5, 1, 2, 3, 4, 24, 48, and 72 h). For assays on the effect of inhibitors of intracellular signaling proteins, cells were preincubated for 2 h with the inhibitors prior to the addition of the anti-CD13 mAb. Aggregation was quantified by light microscopy and is presented as percentage of aggregation (number of cells in aggregates/total number of cells×100). As the size of the cell aggregates after 4 h of incubation made optical quantification impossible, images of each well were captured using a camera attached to a Zeiss Axiovert microscope, and quantification of cells in aggregates was performed using the colony-counting function of Quantity One software (Bio-Rad, Hercules, CA). Data are presented as aggregation indexes (AI) = [number of cells detected by the software as blue colonies in each image (aggregated cells)/total number of cells detected×100]. The effect of inhibitors is expressed as AI percentage of control = AI obtained with the anti-CD13 mAb in the presence of the inhibitor/AI obtained with the anti-CD13 mAb alone (control) × 100. Settings of the software were adjusted to detect as blue colonies all aggregates formed by more than three to four cells, which present optical densities (OD) high enough to avoid erroneous detection of two close cells as aggregates. Thus, AI obtained by quantification with the software are lower than, but comparable with, the percentage of aggregation obtained by visual counting. Both evaluations always correlated consistently. EDTA, sodium azide, colchicine, and 2-deoxyglucose (2-D-glucose) were from Sigma Chemical Co. Herbimycin, genistein, PD98059, Ro-31-8220, bisindolylmaleimide I, SB203580, and LY294002 were from Calbiochem (San Diego, CA).

Competition assays by immunofluorescence

U-937 cells (2.5×10^4) were incubated for 5 min in blocking buffer [phosphate-buffered saline (PBS)/5% FBS/0.1% sodium azide]. Saturating concentrations of the indicated anti-CD13 antibody were added, and cells were incubated for 30 min at 4°C. Saturating amounts of the competing antibody were added, and cells were incubated for another 30 min at 4°C. After washing, a FITC-labeled goat anti-mouse secondary antibody was added for 30 min at 4°C. Cells were fixed in 1% paraformaldehyde and analyzed by flow cytometry.

Enzymatic activity determinations

APN enzymatic activity was determined by the colorimetric measurement of hydrolysis of the substrate L-alanine-p-nitroanilide (H-Ala-pNA; Bachem Biosciences, King of Prussia, PA), as described previously [23]. Briefly, 5×10^5 cells were preincubated with the indicated mAb or inhibitors in PBS with 10% FBS for 1 h at 37°C. Substrate was added to a final concentration of 6 mM for 1 h at 37°C. Cells were pelleted, and the absorbance of the supernatants at 405 nm was determined immediately. Data presented as percentage of the control represent the average absorbance of at least three different experiments performed in triplicates normalized to the control of cells incubated without any mAb or inhibitor previous to incubation with the substrate. The maximal inhibitory dose of bestatin was determined previously to be of 0.4 mg/ml. The protease inhibitor cocktail used as negative control for bestatin (Complete Mini EDTA-free) was from Roche Diagnostics (Indianapolis, IN).

Immunoprecipitation and immunoblot

Aggregated (HA) and nonaggregated (NA) U-937 cells (20×10^6) were washed, resuspended in ice-cold lysis buffer (150 mM NaCl, 10 mM Tris-HCl, glycerol 5%, Brij 97 1%, pH 7.5) with 1 mM phenylmethylsulfonyl fluoride, 10 mM NaF, and 1 μg/ml each aprotinin, leupeptin, pepstatin A, and Na_3VO_4, and kept on ice for 15 min. Lysates were clarified by centrifugation at 14,000 rpm at 4°C for 15 min. Supernatants were incubated overnight at 4°C with 10 μg/ml anti-CD13 452 mAb. Agarose-protein G beads were added to the lysates and incubated for 2 h at 4°C. Beads were washed several times with lysis buffer and resuspended in Laemmli sample buffer. Immunoprecipitates were separated on 10% sodium dodecyl sulfate-polyacrylamide gel electrophoresis and transferred onto nitrocellulose membranes (Bio-Rad) using a semi-dry Trans-blot apparatus (Bio-Rad). Membranes were blocked in 3% bovine serum albumin (BSA) in Tris-buffered saline (TBS) containing 0.05% Tween 20 (T-TBS) overnight at 4°C. After washing, CD13 was detected with 2 μg/ml of the 452 mAb in 3% BSA T-TBS and a secondary horseradish peroxidase (HRP)-conjugated antibody. Chemiluminiscent signal was detected using Super Signal enhanced chemiluminescent kit (Pierce), according to the manufacturer's instructions. The same membranes were stripped with 0.1 M glycine (pH 2.5), blocked for 1 h, and reblotted with an anti-Grb2 or anti-Sos antibody, followed by HRP-conjugated secondary antibody. Detection was made as described above.

Subcellular localization assays by live cell laser scanning confocal microscopy (LSCM)

HA of U-937 cells at a concentration of 2×10^6 cells/ml was performed on glass-bottom culture dishes (MatTek Corp., Ashland, MA) using Texas Red-labeled $F(ab)'_2$ fragments of anti-CD13 mAb. Changes in CD13 localization were imaged by LSCM on a Zeiss LSM 510 META confocal microscope equipped with a Zeiss 37°C incubation system at a 63× magnification. Time-series were obtained with a 2-min delay during the process of aggregation (45 min–1 h). As a control, a FITC-labeled anti-CD11a mAb was used together with the Texas Red-labeled anti-CD13 mAb in some of the experiments. Images were analyzed using the Zeiss LSM Image Examiner.

RESULTS

Anti-CD13 mAb 452 induces HA in a time- and dose-dependent manner

For our initial evaluation of CD13 in monocytic cell adhesion, we used the U-937 cell line as our model system, as it has been studied extensively in HA. To preclude the previously described functional cooperation between Fc receptors for IgG (FcγRs) and CD13 [13], we used $F(ab)'_2$ fragments of the 452 antibody in all experiments. Initial experiments indicated that incubation of U-937 cells with intact anti-CD13 mAb 452 or its $F(ab)'_2$ fragments induced HA (expressed as the percentage of aggregation=the number of cells in aggregates/total number of

cells×100) in a dose-dependent manner (**Fig. 1A**). The percentage of cells in aggregates reached a plateau at antibody concentrations between 0.09 and 3 μg/ml (Fig. 1A) and decreased with higher or lower concentrations. Aggregates were smaller in size at the lowest HA-inducing concentration of the 452 mAb (0.09 μg/ml, Fig. 1A, open arrow). Therefore we chose the minimal dose required to induce aggregates of maximum size as our working antibody concentration throughout the study (3 μg/ml, Fig. 1A, solid arrow). It is important that Fab fragments of the 452 antibody were not able to induce HA of U-937 cells, suggesting the necessity for CD13 cross-linking for the induction of aggregation (not shown).

Aggregation was evident after ~15 min of incubation with the antibody, and ~80% of cells were aggregated after 4–5 h [Fig. 1B, values include smallest aggregates (pairs of cells)]. Incubation periods longer than 4 h yielded large cellular aggregates difficult to quantify by optical microscopy and thus, were quantified digitally (see Materials and Methods). Cellular aggregation peaked after 24 h of incubation with the mAb 452, and cells began to disaggregate after 48 h at 37°C (Fig. 1D). It is important that the rate of HA (and of dissaggregation) is dependent on cell density, as higher concentrations of cells incubated with anti-CD13 mAb aggregate and dissaggregate more rapidly. Thus, at 2×10^6 cells/ml, more than 90% of the cells had aggregated within 1 h of incubation at 37°C (not shown), and by 8 h, aggregation had been lost completely.

HA-inducing capacity of anti-CD13 mAb does not correlate with their ability to inhibit enzymatic activity

A second anti-CD13 mAb (clone WM-4.7) was tested for its capacity to induce HA of U-937 cells. This mAb did not induce HA at any of the concentrations or times of incubation tested (Fig. 1, C and D). As this mAb does not block CD13 enzymatic activity [23], and the effect of the HA-inducing 452 mAb on this activity is not known, the possibility that HA is related to a differential effect of these mAb on CD13 enzymatic activity existed. Thus, to study this hypothesis, we tested two other mAb with defined effect on enzymatic activity: MY7, which is known to partially block APN activity, and WM-15, which has been reported to be a better inhibitor of this activity [23, 24].

The MY7 mAb induced a HA response of U-937 cells, similar to that obtained with the 452 mAb (Fig. 1, C and D). High doses of the MY7 mAb were poor inducers of aggregation, and optimal dose was identical to that of the 452 mAb (0.39 μg/ml, Fig. 1C). AI observed at 4 h with the MY7 mAb were lower than those observed with the optimal dose of the 452 mAb (Fig. 1, C, E, and F). Nevertheless, after 24 h of incuba-

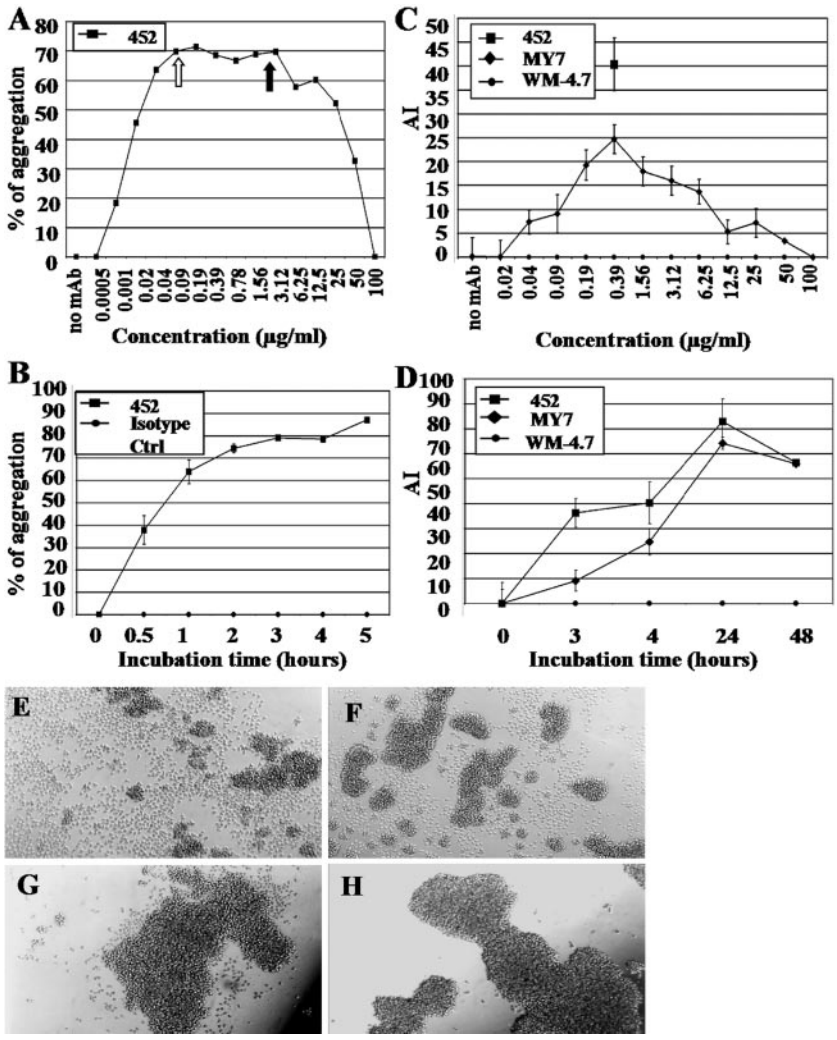

Fig. 1. Dose and time dependence of anti-CD13 mAb-induced HA. (A) U-937 cells in 96-well plates were incubated for 4 h at 37°C with the indicated doses of $F(ab)'_2$ fragments of the anti-CD13 mAb 452. Percentage of aggregation was determined under light microscopy as the number of cells in aggregates/total number of cells × 100. Aggregates were smaller in size at the lowest HA-inducing concentration of the 452 mAb (0.09 μg/ml, open arrow). The minimal dose required to induce aggregates of maximum size was 3 μg/ml (solid arrow). (B) Time-course of anti-CD13 mAb 452-induced HA at the optimal dose (0.39 μg/ml) as quantified under light microscopy (■). As a control, cells were incubated with an isotype-matched mAb (●). (C) HA induced by different anti-CD13 mAb. Cells were incubated with the indicated mAb for 4 h at 37°C. Images were acquired using a camera attached to a Zeiss Axiovert inverted microscope. AI = [number of cells detected by the software as blue colonies in each image (aggregated cells)/total number of cells detected×100] was determined using the colony-counting function of Quantity One software. Optimal dose of the MY7 mAb (♦) was determined to be identical to that of the 452 mAb (■). WM-4.7 mAb (●) did not induce HA at any dose tested. (D) Time-course of HA induced by the indicated mAb at 37°C. WM4.7 mAb did not induce HA at any of the times tested. (E and F) Representative images of HA obtained with MY7 and 452 mAb, respectively, after 4 h of incubation at 37°C. (G and H) HA obtained with the MY7 and 452 mAb, respectively, after 24 h of incubation at 37°C.

tion, the optimal MY7 mAb-induced aggregation had reached similar levels as those obtained with optimal doses of the 452 mAb (Fig. 1, D, G, and H). The WM-15 mAb was also able to induce HA, although at lower levels than those induced by the 452 and MY7 mAb (not shown).

To rule out the possibility that the differences in the ability of the four mAb to induce HA were related to differences in binding to U-937 cells, we measured antibody binding by flow cytometry (**Fig. 2**). As a result, each of the antibodies was fully able to bind to the cells to a similar degree excluding that possibility.

To determine if our results on antibody-induced HA correlated with CD13 enzymatic activity, we measured aminopeptidase activity in the presence of each of the antibodies (**Fig. 3A**). As a control, we used bestatin, a well-known inhibitor of aminopeptidase activity, which preferentially targets CD13 in the cell membrane [25]. As optimal induction of HA occurs at subsaturating antibody concentrations, we measured activity at saturating and optimal HA doses. As previously reported for myeloid cell lines [24], saturating concentrations of the WM-4.7 mAb had no effect on cell-surface CD13 enzymatic activity (Fig. 3A, WM-4.7^s), MY7 and 452 had a small but significant effect (MY7^s, 452^s), and bestatin and WM-15 mAb (WM-15^s) inhibited activity by ~50% (residual enzyme activity is a result of other peptidases on the cell surface) [24]. In contrast, at doses optimal for HA induction, none of the aggregation-inducing mAb inhibited enzymatic activity (452^{HA}, MY7 ^{HA}, and WM-15^{HA}, Fig. 3A). In addition, chemically blocking enzyme activity with inhibitory doses of bestatin neither induced aggregation nor affected HA induced by the 452 mAb (not shown). Furthermore, as shown later, EDTA, which is an irreversible inhibitor of APN enzymatic activity, had no effect on CD13-mediated HA either. Taken together, these results indicate that anti-CD13-induced HA is independent of CD13 enzymatic activity.

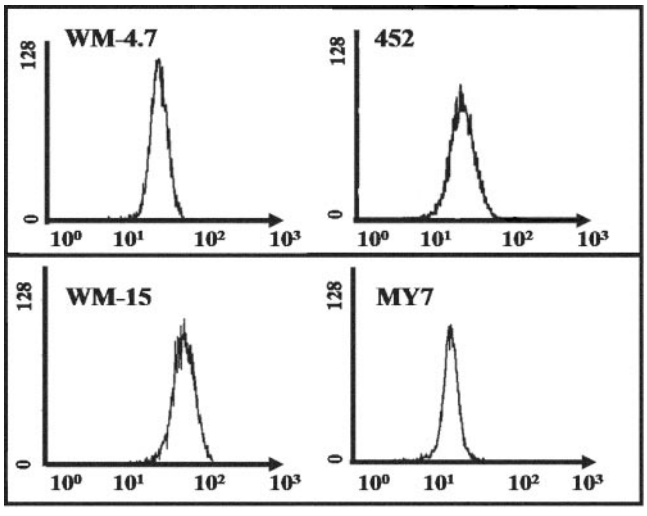

Fig. 2. Capacity of mAb to induce aggregation does not depend on differences in their binding patterns. Binding of the indicated anti-CD13 mAb (2.5 μg/0.5 ml) to U-937 cells was determined using indirect immunofluorescence by flow cytometry. A histogram of a representative experiment with the indicated anti-CD13 mAb is shown.

Binding to specific epitopes on CD13 is important for the induction of HA

As CD13 enzymatic activity appeared to be unrelated to induction of aggregation, we further tested a possible relationship between the epitope recognized by each mAb and its ability to induce HA. The binding sites of two of the three HA-inducing mAb are known: WM-15 binds to the zinc-binding domain of the enzyme, and MY7 binds to an epitope distinct but close to this domain [3, 23]. The binding epitope of the other HA-inducing mAb, 452, is not known. WM-4.7 mAb, which is unable to induce HA, is known not to bind to the zinc-binding domain [23]. With these data in mind, we carried out competition assays by flow cytometry. Preincubation of U-937 cells with the 452 mAb efficiently blocked the subsequent binding of the MY7 mAb, suggesting that the epitopes recognized by both mAb are the same or close to one another (Fig. 3B). In contrast, preincubation of cells with the 452 mAb did not interfere with binding of the WM-4.7 mAb (Fig. 3C). Binding of the WM-15 mAb was not blocked by the 452 mAb (Fig. 3D) or by the MY7 mAb (not shown). Thus, as the epitopes recognized by WM-15 and MY7 (and consequently, 452) mAb are known to be closely located [23], these results suggest that the HA-inducing capacity of the three mAb depends on their binding to a specific site, which lies close to the enzymatic active site of CD13.

Membrane expression of CD13 and adhesion molecules during HA

To determine the effect of HA on surface expression of CD13 and the adhesion molecules CD18, CD11a, CD29, and CD54, we assayed aggregated and NA cells by flow cytometry. A decrease in the membrane expression of CD13 could be seen on aggregated cells as compared with NA cells. No change in the membrane expression of the other molecules was observed (**Fig. 4**). These results suggest that CD13-mediated HA does not depend on an increase in membrane levels of the integrins tested.

Effect of antibodies against CD29, CD11a, CD18, CD54, and CD98 on CD13-induced aggregation

Despite the fact that surface expression of adhesion molecules was not altered by CD13-induced HA, it was still possible that they play a direct role in the adhesion phenomenon. Therefore, we tested possible inhibition of aggregation by specific mAb.

Coincubation with anti-CD11a, CD18, CD54, or CD98 mAb had no statistically significant effect on the aggregation induced by CD13 at any time or concentration tested (**Fig. 5A**). On the contrary, as early as after 2 h of incubation, treatment with anti-CD29 mAb markedly increased CD13-induced aggregation up to an AI of 201.8% ± 15.4 of that observed by anti-CD13 mAb alone (not shown). After 4 h, anti-CD13 aggregation in the presence of anti-CD29 mAb was 80.9% higher than that induced by the anti-CD13 mAb alone. However, after 24 h, cells aggregating in the presence anti-CD13 alone, reached the same levels of aggregation as those with the combination of anti-CD29 and anti-CD13 mAb (Fig. 5A). After 48 h, the anti-CD13 mAb-induced aggregation begins to decrease (Fig. 5B) until it disappears at 72 h (Fig. 5C). However,

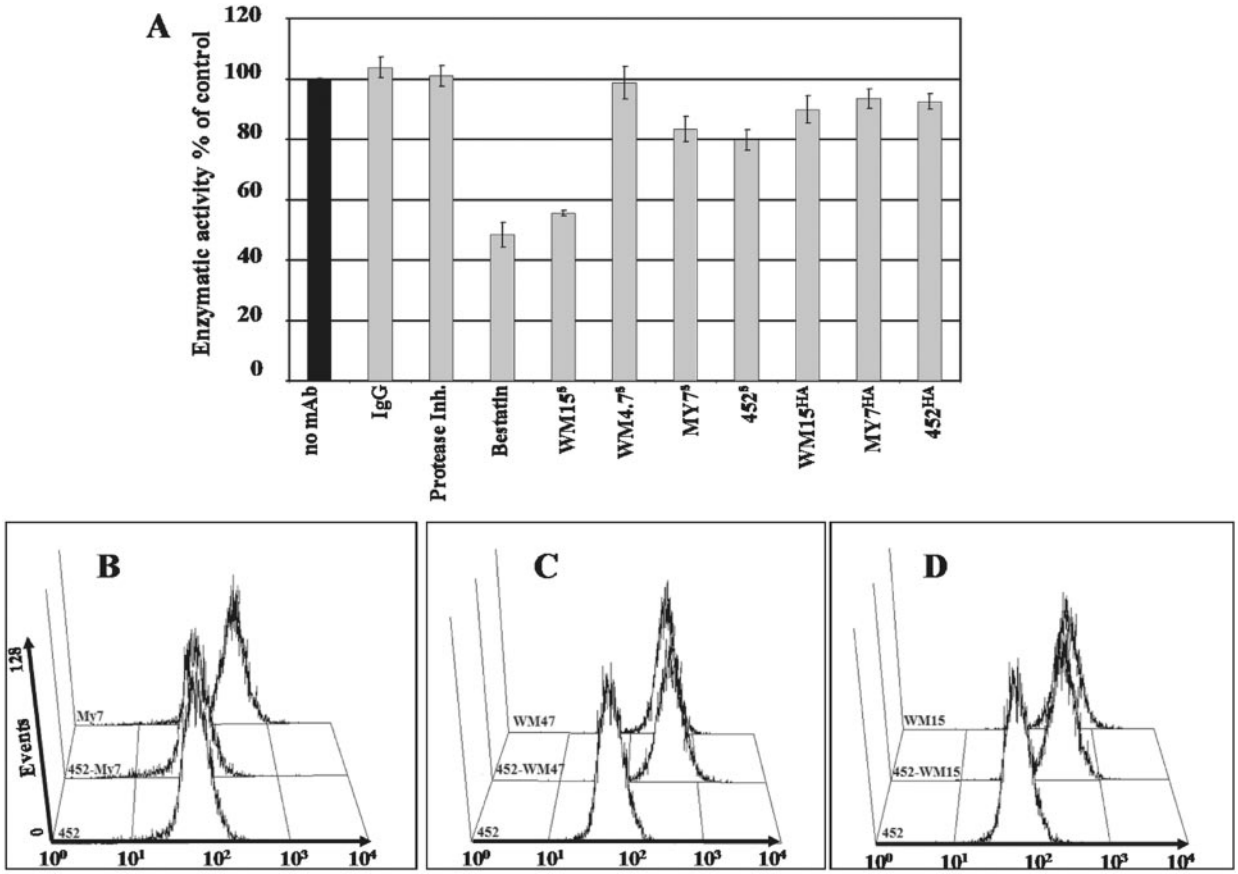

Fig. 3. HA-inducing capacity of anti-CD13 mAb does not correlate with their ability to inhibit enzymatic activity but correlates with specificity of binding. (A) Cells (5×10^5) were incubated with the indicated antibodies or inhibitors for 1 h at 37°C. Substrate (H-Ala-pNA) was added at a final concentration of 6 mM and further incubated for 1 h at 37°C. Cells were pelleted, and OD_{450} was determined in the supernatants. Percentage of OD values as compared with the control without antibodies or inhibitors (no mAb) is shown. Bestatin was used at a concentration of 0.4 μg/ml. ^{s} = Saturating concentrations; ^{HA} = optimal dose for HA of the indicated mAb. (B, Front histogram) U-937 cells were incubated at 4°C with the HA-inducing mAb 452 for 30 min. After washing, a secondary FITC-labeled antibody was added and incubated for 30 min. Cells were fixed and analyzed by flow cytometry. (Middle histogram) After the first 30 min with the 452 mAb, the MY7 mAb was added for another 30 min at 4°C. After washing, incubation with secondary antibody and fixation was carried out as before. (Rear histogram) Cells were incubated for 30 min with the MY7 mAb only. The higher fluorescence intensity observed with the MY7 mAb alone was blocked by preincubation with the 452 mAb. (C) Same protocol as in B but using the NA-inducing clone WM-4.7. In this case, the higher fluorescence peak obtained with the WM4.7 mAb alone was not inhibited by preincubation with the 452 mAb. (D) Same protocol as in B but using WM-15 mAb. 452 mAb did not block binding of this mAb.

in the presence of the anti-CD29 mAb alone or in combination with the anti-CD13 mAb, cells remained aggregated at these incubation times (Fig. 5D). The anti-CD29 mAb (clone 4B4), but not any other anti-integrin mAb used, was able to induce HA of U-937 cells on its own (see **Fig. 6B**) with similar kinetics as those observed when coincubated with the anti-CD13 mAb (not shown), suggesting that this prolonged aggregation could be dependent on the CD29-induced HA rather

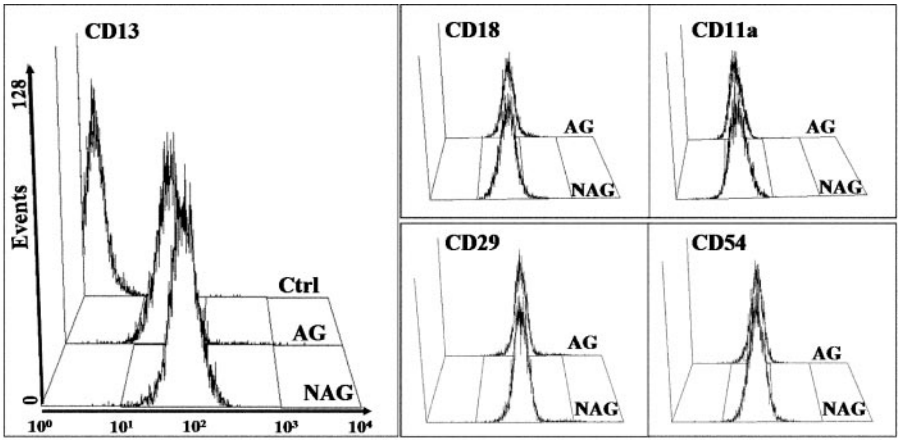

Fig. 4. CD13 but not integrin membrane expression is down-regulated during HA. Membrane expression of the indicated molecules was determined by flow cytometry after 24 h of incubation, with or without the anti-CD13 mAb 452, using FITC-labeled, specific mAb. Front histograms represent expression on NA cells (NAG). Rear histograms represent expression on aggregated cells (AG). Leftmost histogram on the CD13 panel represents the control of cells incubated with an isotype-matched, FITC-labeled antibody (Ctrl).

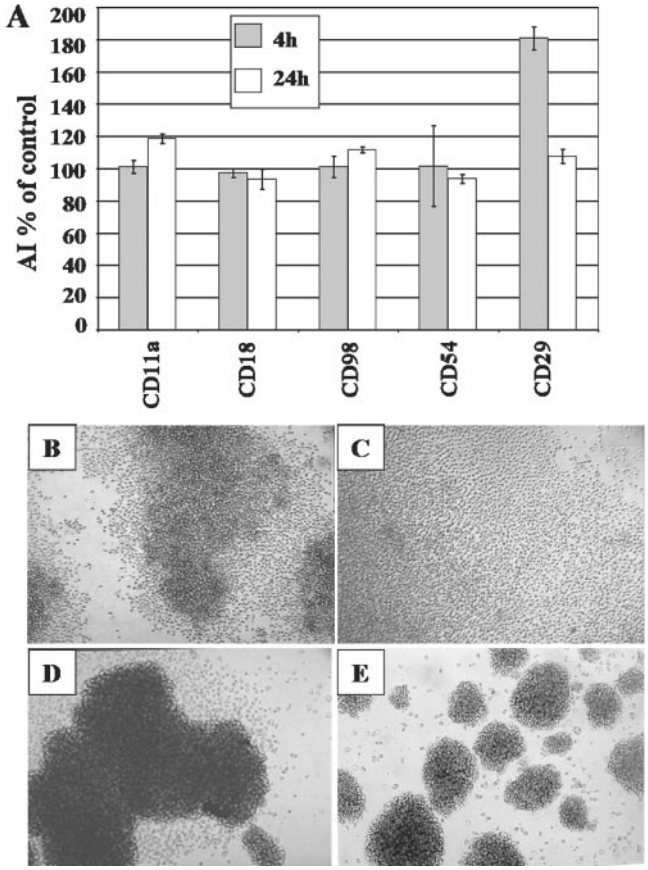

Fig. 5. mAb against adhesion molecules do not inhibit CD13-induced HA. (A) Cells were incubated with anti-CD13 mAb 452 in the presence of different doses of the indicated antibodies for 4 h (shaded bars) or 24 h (open bars) at 37°C. As no effect on CD13-mediated HA was observed at any of the concentrations tested, AI obtained with saturating doses of the antibodies, as determined by flow cytometry, were used for the graph. Except for the anti-CD29 mAb, none of the indicated mAb induced HA in the absence of the anti-CD13 mAb. (B) HA obtained with the anti-CD13 mAb 452 alone at 48 h of incubation. (C) HA obtained with the 452 mAb alone at 72 h of incubation. (D) HA obtained at 48 h by coincubation of the 452 with the anti-CD29 mAb. (E) HA obtained at 48 h by coincubation of the 452 with the CD11a mAb.

than a synergistic effect between CD13 and CD29. Finally, the decrease in CD13-induced cellular aggregation after 48 h (Fig. 5B) was also prevented by anti-CD11a (Fig. 5E) and anti-CD54 mAb (not shown), resulting in aggregates which persisted up to 96 h of incubation. These results suggest that although anti-CD13 mAb-induced aggregation appears to be independent of integrins, ligation of these molecules can increase it, apparently by stabilizing the cellular aggregates induced by anti-CD13.

Metabolic requirements of CD13-induced aggregation

HA is a dynamic process, which involves metabolically active cells. To determine the metabolic pathways participating in CD13-induced aggregation, we tested the effect of several metabolic inhibitors on this process. As integrin-mediated adhesion is strictly dependent on calcium, we initially assessed this aspect by removal of free calcium from the media by EDTA. As shown in Figure 6A, CD13-induced aggregation was not inhibited significantly by any of the concentrations of EDTA tested, while the anti-CD29-induced HA was inhibited completely by EDTA at the same concentrations (Fig. 6B) as previously reported [18].

Similarly, we tested inhibitors of glycolysis (2-D-glucose) and electron transport in the respiratory chain (sodium azide). Blocking glycolysis inhibited aggregation by 99.01% (Fig. 6A), and electron transport did not appear to be necessary for CD13-induced HA. The energy dependence of anti-CD13-induced HA was supported further by its dependence on temperature, as incubation at 4°C completely abrogated anti-CD13 mAb-induced aggregation (not shown).

Finally, to determine the contribution of microtubules in anti-CD13 mAb-induced HA, we added the microtubule polymerization inhibitor colchicine to our assay. CD13-dependent HA was significantly higher in the presence of all doses of colchicine tested (Fig. 6C). This effect was present throughout the experiment; however, it was more evident at the shorter times before anti-CD13-induced HA had reached its maximum. Doses of colchicine up to 30 μM had the same synergistic effect (not shown). These results suggest that CD13-mediated HA is an active, energy-dependent process, which is integrin-independent and in which microtubules play an important and apparently inhibitory role.

Effect of kinase inhibitors on CD13-mediated HA

As the results obtained with metabolic inhibitors suggested that CD13-mediated HA is an active and possibly signal transduction-dependent phenomenon, we tested several chemical inhibitors of intracellular kinases. It had been reported that CD13-induced signal transduction in monocytic cells involves tyrosine kinases (especially *Src*), phosphatidylinositol-3 kinase (PI-3K) and mitogen-activated protein kinases (MAPK), extracellular signal-regulated kinase (ERK)1/2 and p38 [26]. Here, we tested the following inhibitors: herbimycin (*Src* kinases), genistein (tyrosine kinases), PD98059 [MAPK kinase (MEK)-1], LY294002 (PI-3K), SB203580 (p38), Ro-31-8220, and bisindolylmaleimide I [protein kinase C (PKC)]. Cells were preincubated for 2 h with a range of at least eight different concentrations of each inhibitor before the addition of the anti-CD13 mAb. AI was determined at 4 and 24 h at the concentrations of inhibitors at which cell viability was not affected. The whole range of concentrations was tested in at least three independent experiments, and representative results are shown in **Figure 7A**. The most prominent effect was obtained with herbimycin, which completely inhibited CD13-mediated HA, suggesting that *Src* kinases are indispensable for the process. Inhibitors of PI-3K, MEK-1, and p38 also inhibited HA importantly (79.39±5.01%, 91.90±0.18%, and 68.5 ± 7.2%, respectively). Genistein inhibited HA in 35.88% ± 3.92, and the lowest inhibitory effect was obtained with the PKC inhibitors bisindolylmaleimide I and Ro-31-8220 (48.72% and 43.10%, respectively). These results support the involvement of MAPK in CD13-induced HA. As Grb2 is a common upstream adaptor protein involved in the ERK1/2 MAPK signaling pathway, we tested a possible physical association between CD13 and Grb2, which binds to phosphorylated tyrosine residues through its Src homology 2 domain. Sos is a guanosine 5′-diphosphate-guanosine 5′-triphosphate ex-

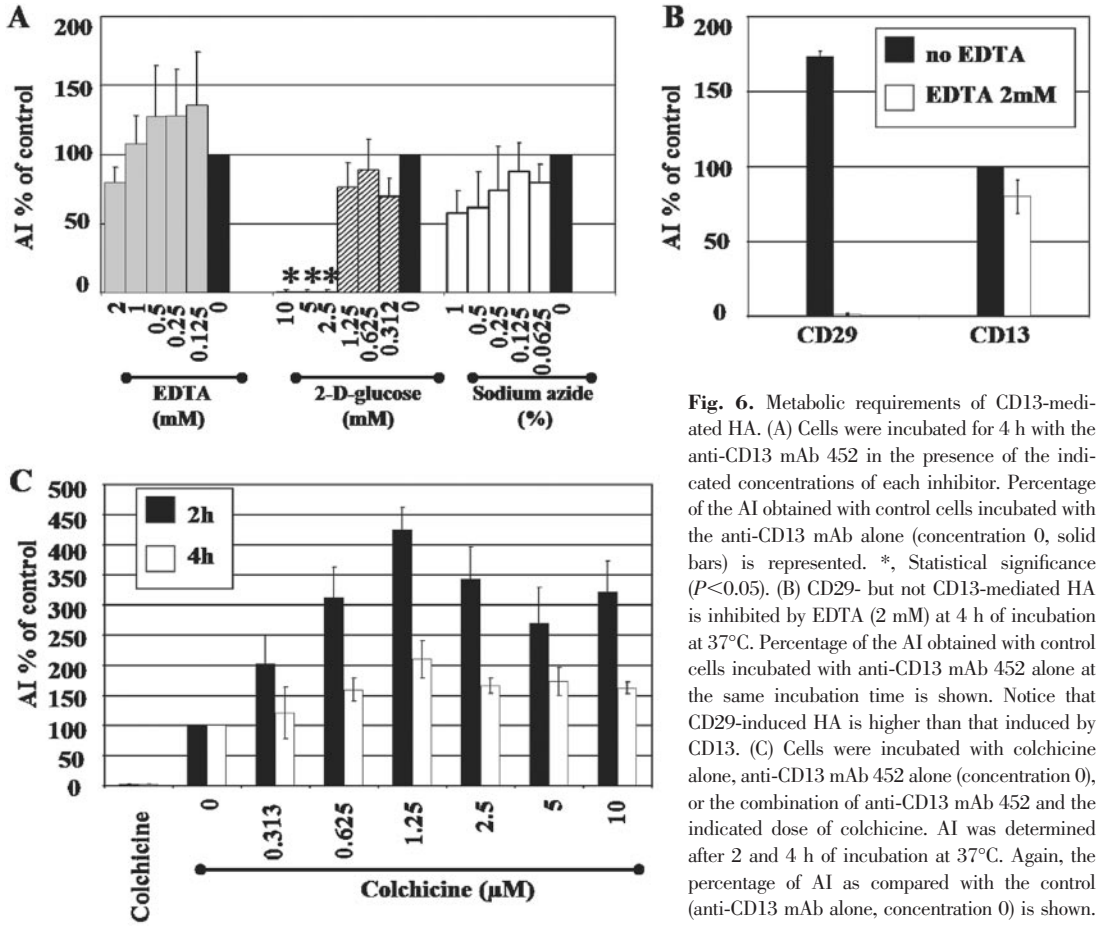

Fig. 6. Metabolic requirements of CD13-mediated HA. (A) Cells were incubated for 4 h with the anti-CD13 mAb 452 in the presence of the indicated concentrations of each inhibitor. Percentage of the AI obtained with control cells incubated with the anti-CD13 mAb alone (concentration 0, solid bars) is represented. *, Statistical significance ($P<0.05$). (B) CD29- but not CD13-mediated HA is inhibited by EDTA (2 mM) at 4 h of incubation at 37°C. Percentage of the AI obtained with control cells incubated with anti-CD13 mAb 452 alone at the same incubation time is shown. Notice that CD29-induced HA is higher than that induced by CD13. (C) Cells were incubated with colchicine alone, anti-CD13 mAb 452 alone (concentration 0), or the combination of anti-CD13 mAb 452 and the indicated dose of colchicine. AI was determined after 2 and 4 h of incubation at 37°C. Again, the percentage of AI as compared with the control (anti-CD13 mAb alone, concentration 0) is shown.

change protein that binds Grb2 through proline-rich sequences, providing a link between Grb2 and MAPK, usually through the activation of Ras. As shown in Figure 7B, Grb2 and Sos coimmunoprecipitate with CD13 from lysates of resting and aggregated U-937 cells, further supporting the use of this signaling pathway by CD13 in monocytic cells. A lower amount of Grb2 and Sos was found to coprecipitate with CD13 from lysates of aggregated cells than from resting cells. The significance of the observed decrease in the association of Grb2 and Sos with CD13 after HA is, at present, unknown. As mentioned above, at high cellular densities, the aggregation and disaggregation phenomena occur faster. Thus, the observed decrease in the association of Grb2 and CD13 could probably be related to the disaggregation process. Figure 7C depicts a hypothetical signaling cascade, which may occur after CD13 cross-linking on the cell membrane according to the data presented here, which coincide with the previous report of Santos et al. [26].

CD13 redistributes to the zones of cell-cell contact during HA of U-937 cells

Next, we wished to determine the subcellular localization of CD13 molecules during aggregation. HA was induced with Texas Red-labeled $F(ab)'_2$ fragments of anti-CD13 mAb 452, and CD13 distribution during the process of aggregation was followed with time-lapse LSCM at 37°C. As shown in **Figure 8** and in the supplemental video created with the individual images of the time series, during HA, CD13 polarizes and accumulates at the zones of cell-cell contact, and the majority of the CD13 signal is localized in these zones once aggregation has been completed. As a control, in some experiments, a FITC-labeled anti-CD11a mAb was added along with the Texas-Red-labeled anti-CD13 mAb, and no change in the membrane distribution of CD11a was seen even after aggregation was complete (Fig. 8, last image). These results suggest that CD13 actively participates in the aggregation process.

DISCUSSION

Homotypic and heterotypic adhesion between cells is extremely important for many physiological and pathological processes. Changes in the adhesive properties of cells are often a result of specific alterations in the levels of expression or in the affinity of adhesion molecules. These alterations can occur in response to diverse external stimuli, such as soluble factors or those encountered during cell-cell and cell-matrix contacts. The study of HA in vitro is a useful model to investigate the molecular mechanisms regulating these alterations in response to specific stimuli.

We have found that certain anti-CD13 mAb are able to induce HA of the promonocytic cell line U-937, and others have no effect. Most of the functions so far attributed to CD13 have been reported to depend on its enzymatic activity. Thus, the observed differences in the ability of anti-CD13 mAb to

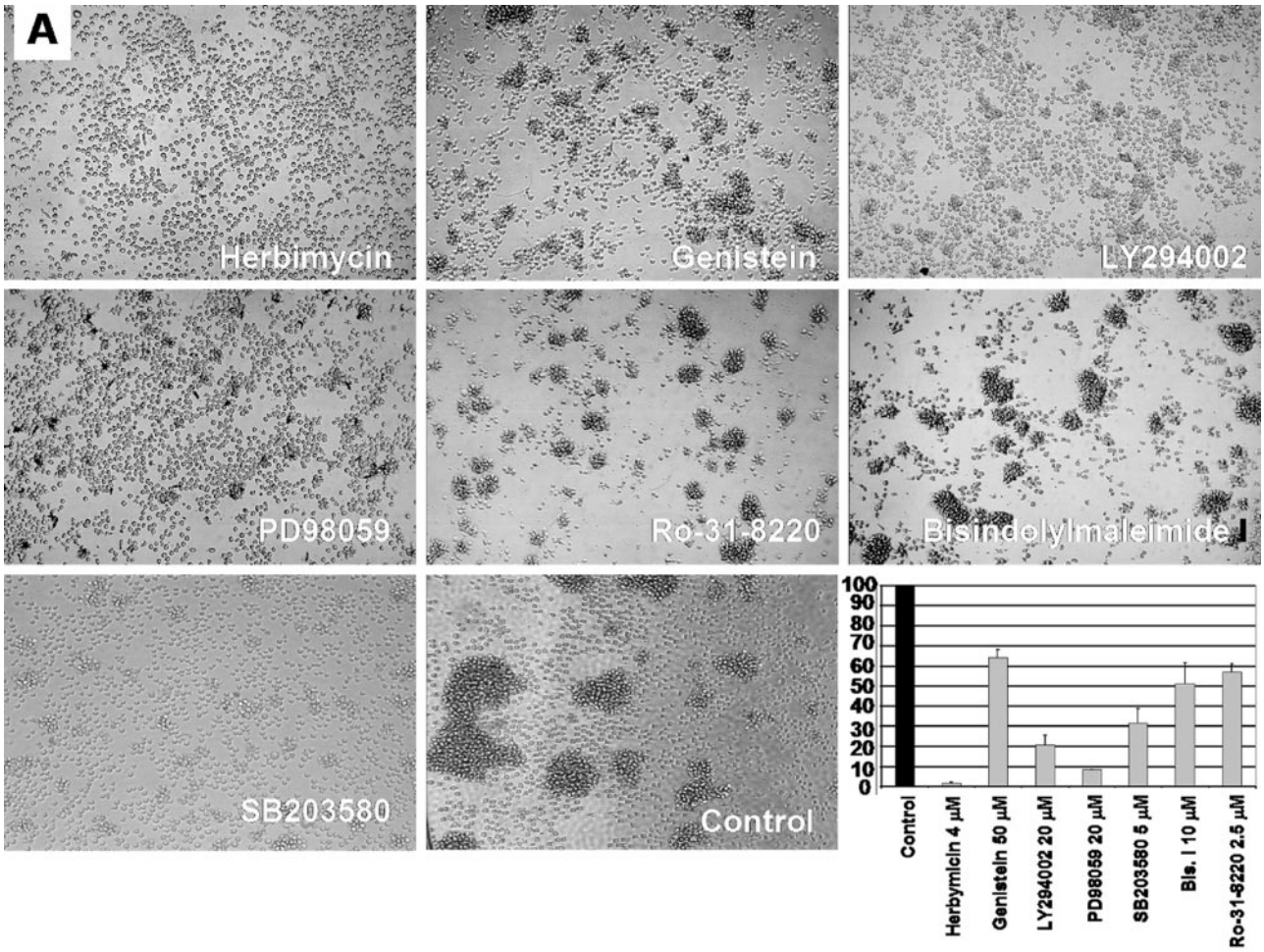

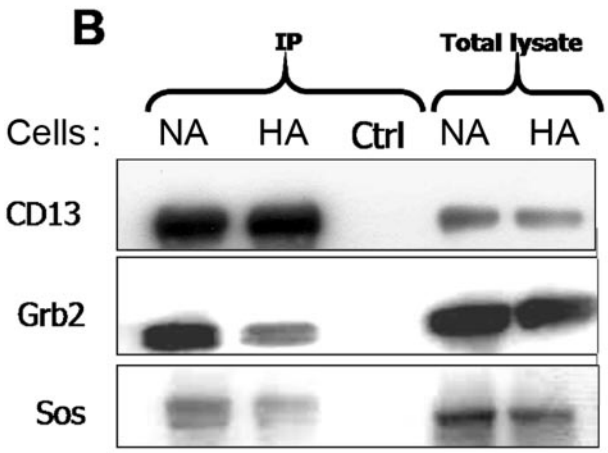

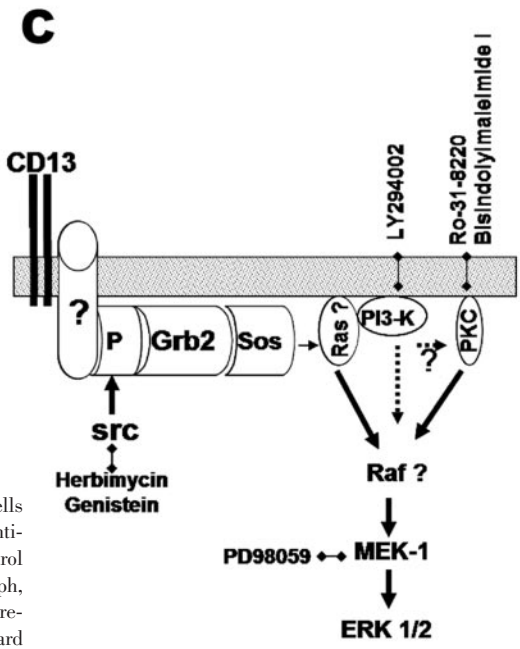

Fig. 7. Signal transduction involved in HA induced by anti-CD13 mAb. (A) Cells were preincubated for 2 h with the indicated inhibitor. Subsequently, the anti-CD13 mAb 452 was added, and the pictures were taken 4 h later. The control picture shows the aggregation obtained in the absence of inhibitors. In the graph, the percentage of the AI obtained with control cells (Control, solid bar) is represented for the indicated dose of each inhibitor (shaded bars, mean and standard deviation of at least two independent experiments). (B) HA was induced with the optimal dose of the 452 mAb using 8×10^6 cells/ml. Cells (20×10^6) were lysed after 60 min at 37°C. An identical amount of cells was incubated in parallel at the same conditions (cell density, temperature, time) but without anti-CD13 antibody (lanes labeled NA). CD13 was immunoprecipitated (IP) from lysates of NA and aggregated (HA) cells, as described in Materials and Methods. Ctrl lane corresponds to an immunoprecipitate from lysates of NA cells carried out with an irrelevant, isotype-matched antibody. An anti-CD13 immunoblot was performed using the same mAb 452 (top panel, CD13), and subsequently, the same membrane was blotted for Grb2 and Sos (middle and bottom panels). For the identification of the corresponding bands, total lysates of each sample were included. (C) A hypothetical signal transduction pathway, induced by CD13 cross-linking by mAb on the monocytic cell membrane, is depicted, according to our data about coimmunoprecipitation and kinase inhibitor's effect. P = Phosphotyrosine

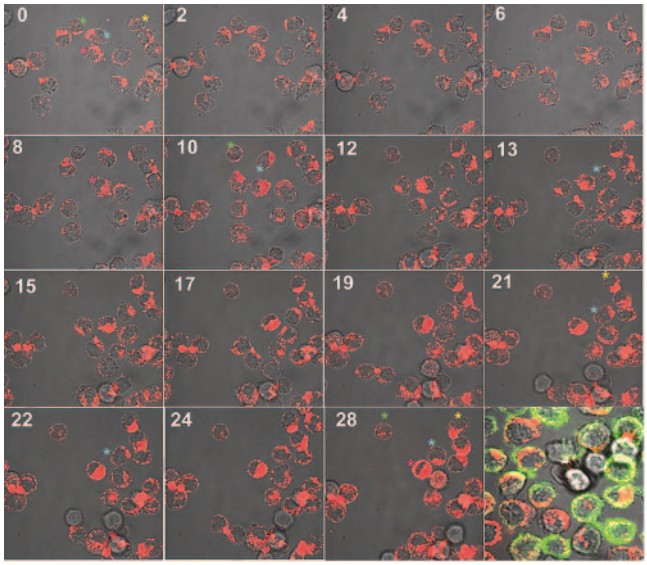

Fig. 8. CD13 relocates to the zones of cell-cell contact during HA. U-937 cells were incubated with Texas Red-labeled anti-CD13 mAb 452 (0.39 μg/ml) in a glass-bottom culture dish in RPMI-1640 phenol red-free complete medium. Time-lapse imaging at 2-min intervals was performed in a Zeiss LSM 510 META confocal microscope equipped with a Zeiss heater temperature control system and including an objective heater (original magnification, ×63). Images were analyzed and exported using the Zeiss LSM Image Browser 3.5.0.223. Numbers represent the incubation time in minutes. Time 0 corresponds to 10 min of incubation at 37°C with the mAb before the beginning of imaging. The cell indicated by the green asterisk relocates CD13 to the zone of its membrane, which is closer to the two surrounding cells; however, as soon as those cells begin to migrate away, polarization of CD13 is lost. The cell marked by the blue asterisk polarizes CD13 to the zone of its membrane, where it starts to approach the surrounding cells, that proximity is lost (4-min image), and the cell turns clockwise (10-min image) until it relocates the zone of polarized CD13 toward its new aggregation partners (28-min image). The cell marked by the white asterisk progressively moves from the center of the field toward the aggregate, showing increasing levels of CD13 polarization along the way. At 10 min of incubation, one cell approximates to its left, and it turns counter-clockwise, showing CD13 polarized to that side at 13 min. As this contact is not established, it turns clockwise again until it ends, establishing contact with the rest of the main aggregate at the right half of the field. The cell marked by the yellow asterisk is clearly not polarized at the beginning of incubation, but as soon as it makes contact with its aggregation partner, it starts turning counter-clockwise, until at the end of incubation, it shows CD13 completely polarized to the zone of cell-cell contact. Finally, the cell marked with the green asterisk polarizes CD13 during the period of time at which it is in close proximity with other cells. However, as the other cells move away, this cell loses its polarity and stays in the same place during all the incubation. This indicates that movement of cells does not occur at random. As a control, a FITC-labeled anti-CD11a was used during anti-CD13-induced HA, and no redistribution of CD11a was seen at any time of incubation (last image).

induce HA could be related to their distinct effect on APN activity. However, our results would argue that HA occurs independently of CD13 enzymatic activity for several reasons. First, the two anti-CD13 mAb with the highest capacity to induce aggregation (452 and MY7) have little effect on the enzymatic activity at saturating concentrations or most importantly, at optimal doses for induction of HA. Second, the high concentrations of the WM-15 mAb required to inhibit enzymatic activity do not induce HA. However, this mAb induces HA at lower concentrations, which have no effect on APN activity. Third, the aminopeptidase inhibitor bestatin neither induces aggregation nor blocks HA induced by the 452 mAb at doses at which it inhibits enzymatic activity in these cells. Finally, CD13-mediated HA is insensitive to EDTA, which is an irreversible inhibitor of zinc-dependent APN enzymatic activity [27, 28]. Therefore, CD13-induced monocytic aggregation appears to be independent of enzymatic activity. Similarly, CD13 enzymatic activity is not required for its role as a viral receptor [29, 30], suggesting that this surface molecule may have an array of functions that are independent of its enzymatic activity.

As enzymatic activity did not appear to correlate with CD13-induced HA, we hypothesized that differences in the capacity of the four mAb to induce HA could be related to their binding to specific epitopes on CD13. In support of this theory, competition experiments revealed that the 452 mAb binds to an epitope overlapping with that recognized by the MY7 mAb. Previous epitope mapping studies have shown that MY7 and WM-15 mAb bind to different but closely located epitopes, which lie near the enzymatic active site [23], suggesting that binding to a specific site on CD13 close to the active center is necessary to induce aggregation. Accordingly, the WM-4.7 mAb, which is known to bind to an epitope distinct from the zinc-binding domain and different from that recognized by the HA-inducing mAb, does not induce HA. Furthermore, the MY7 and WM-15 mAb, but not the WM-4.7 mAb, block binding of the human coronavirus 229E to CD13 [3, 29, 30], again supporting the conclusion that both mAb bind to closely spaced epitopes. It is interesting that it has been reported that binding of the anti-CD13 F23 mAb (which is blocked by the WM-15 mAb) induces a conformational change in the extracellular domain, resulting in the exposure of cryptic epitopes [31]. Therefore, it is possible that binding and cross-linking of CD13 by the aggregation-inducing mAb could trigger a proadhesive signal transduction cascade and a conformational change, which results in the exposure of a cryptic epitope responsible for binding or dissociation of an adhesion-related ligand.

As the majority of previous studies implicates integrins as critical mediators of HA, it was possible that one of the consequences of the CD13 cross-linking by mAb was the induction of the expression of integrins. Thus, we evaluated possible changes in integrin expression and possible cross-inhibition of CD13-mediated HA by integrin-specific antibodies. As opposed to HA mediated by CD29 [14], CD43 [19], or phorbol 12-myristate 13-acetate [32], CD13-mediated aggregation is independent of the integrins lymphocyte function-associated antigen-1/intercellular adhesion molecule-1 (CD11a-CD18/CD54) and CD29. The expression of these molecules was unchanged during CD13-induced aggregation, and the respective mAb did not have a significant inhibitory effect on it. On the contrary, antibodies directed against CD29, CD11a, and to a lesser extent CD54, appeared to stabilize cellular aggregates, as they remained intact for longer periods of time. We used an anti-CD29 mAb capable of inducing a HA response that lasted up to 96 h (not shown). This suggests that aggregation induced by the anti-CD29 mAb alone is more stable, and thus, in the presence of both mAb, the longer duration and the increase in CD13-induced aggregation may be the result of the sum of two independent phenomena. Con-

versely, neither the anti-CD11a nor the anti-CD54 mAb used had the property of inducing aggregation by itself (Fig. 5A), which rather suggests a stabilizing effect of these molecules after ligation by the specific antibodies. As EDTA blocks integrin-mediated adhesion, the observation that EDTA has no effect on CD13-mediated HA further supports the conclusion that this phenomenon does not depend on integrins.

In the absence of integrin involvement, the possibility existed that CD13-mediated aggregation was the result of a passive process as a result of a lectin-like agglutination of cells rather than an active, energy-dependent process. To answer this question, we tested the effect of temperature, 2-D-glucose, and sodium azide on CD13 mAb-induced aggregation. Incubation of cells in the presence of optimal doses of the aggregation-inducing antibodies at 4°C completely abrogated aggregation. In addition, 2-D-glucose at the concentrations commonly used to block glycolysis had a clear, inhibitory effect on aggregation. These results suggested that CD13-mediated HA is an active and energy- and probably signal transduction-dependent process. The MY7 and WM15 mAb had been shown to trigger signal transduction involving tyrosine and MAPK in U-937 cells [26]. Our results show that the 452 mAb is also able to trigger a signal transduction cascade, which most probably, is involved in HA. The data obtained with chemical inhibitors clearly implicate tyrosine kinase and MAPK pathways in the signaling cascade involved in HA. The involvement of tyrosine kinases in the process, demonstrated here by inhibition of the HA by herbimycin and by the partial inhibition by genistein, suggested that the Grb2/Sos/Ras/MAPK pathway was involved. Here, we show that the two upstream components of this signaling cascade, Grb2 and Sos, coprecipitate with CD13 in monocytic cells. We have found a constitutive association among these molecules, which persists during aggregation and decreases when cells start to disaggregate. The link between CD13 and Grb2 is still to be identified. As part of the population of CD13 resides in lipid rafts, and the adaptor linker for activation of T cells (LAT) is highly enriched in these domains in monocytic cells, the possibility of this protein being the bridge between CD13 and the MAPK pathway can be proposed. New experiments are necessary to test this hypothesis.

The fact that sodium azide, which blocks electron transport in the respiratory chain, did not significantly inhibit aggregation suggests that CD13-mediated HA can proceed in conditions of anaerobic glycolysis under which most tumor cells grow.

It is important that the microtubule polymerization inhibitor colchicine had an unexpected, synergistic effect on CD13-mediated HA. An increase in AI was observed from the shorter incubation times (Fig. 6C), and longer incubation produced an effect similar to that observed after coincubation with anti-integrin mAb, which is sustained aggregation at time-points in which cells incubated with anti-CD13 mAb alone had started to disaggregate. This result is in keeping with reported results indicating that colchicine and nocodazole (another regulator of microtubule dynamics) increase mobility and activation of integrins and that nocodazole alone induces aggregation of the macrophage cell line J774 [33], although colchicine did not induce aggregation of U-937 cells in our hands. Although our current results strongly suggest that CD13-mediated aggregation is independent of integrins per se, the stabilization in the cellular aggregates at long periods of incubation observed by coincubation with anti-integrin antibodies could be similar and perhaps even related to the effect observed with colchicine. It is also tempting to propose that a distinct type of microtubule-dependent mechanism operates during HA, for example, a similar release of CD13 from cytoskeletal constraints with a consequent increase in its mobility in the cell membrane. When comparing CD13-mediated aggregation with aggregation induced by other molecules in U-937 cells, it is interesting that the same doses of colchicine, which enhanced aggregation induced by CD13, block aggregation mediated by CD98 and CD29.

Finally, the active redistribution of CD13 to the zones of cell-cell contact observed during live cell imaging suggests a direct role of CD13 in the aggregation phenomenon. Polarization of CD13 in the direction of migration implies its participation in the active cellular movement toward the zone of the culture dish where an aggregate is being organized, as well as in the establishment of the cell-cell interaction itself. The fact that CD13 is polarized only when cells are in close proximity further strengthens this conclusion. Also, CD11a, which stabilizes the CD13-induced cellular aggregates at long incubation times, does not redistribute to the zones of cell-cell contact, demonstrating that the CD13 redistribution observed is specific and not dependent on bivalent antibody-mediated cross-linking. Although our results demonstrate an important role for CD13 in cell adhesion, they do not necessarily imply that CD13 itself is the adhesion molecule. As mentioned above, cross-linking of CD13 may only trigger the proadhesive mechanism involving distinct adhesion-related molecules.

In conclusion, we have demonstrated an adhesion-related phenomenon that is CD13-mediated and that can be quantified easily. Future work will focus in determining the molecular mechanisms directing this process and its possible physiological and physiopathological implications. For example, CD13 and several molecules known to mediate HA have been shown to participate in immune responses, as anti-CD13 mAb block dendritic cell (DC)-mediated T cell activation in vitro [34]. In light of our data, it is tempting to propose a role for CD13 in the stabilization of such cell-cell interactions. Under these circumstances, CD13 could act as a signal regulator [35] or costimulatory molecule, which by definition, decreases the threshold for activation of the immunoreceptor by stabilizing cell-cell contacts and/or increasing the presence of the receptor in signal-controlling membrane domains (i.e., lipid rafts), as we have proposed to occur during FcγR-mediated functions [13, 35]. In other cell types, HA also has an important role. Thus, in DC, HA has been shown to be a mechanism of intercellular communication involved in the interchange of maturation signals and in antigen transfer [36]. It is interesting that DC have been shown to express high levels of CD13, and CD13 participates in DC maturation [34, 37–39]. Thus, it could be interesting to determine the relationship between CD13-mediated HA and maturation. Another cell type in which HA plays key roles is neutrophils. In these cells, HA occurs upon activation and is of great relevance in many processes, such as acute inflammation and acute coronary syndromes [40, 41]. CD13

has been shown to participate in both processes. Finally, because of the role of CD13 as a viral receptor [3, 4], it would also be interesting to determine the implications of CD13-mediated aggregation in viral infection-related cell fusion and syncitium formation. It is interesting that the mAb that induce HA are the ones reported to block viral infection [29, 30], and the mAb that does not induce HA is known not to inhibit viral infection.

In this light, elucidation of the role of CD13 in cell adhesion may contribute significantly to our understanding of the numerous critical processes where cell-cell interactions must be regulated precisely.

ACKNOWLEDGMENTS

This work was supported by grants from PAPIIT-Universidad Nacional Autónoma de México (UNAM; IN 220705) and CONACYT (45092) to E. O. and from National Institutes of Health (R01CA106345) and the Susan G. Komen Foundation (BCTR0402745) to L. H. S. P. M-O. was supported by a fellowship from Dirección General de Estudios de Posgrado, UNAM. We thank Dr. Meenhard Herlyn from The Wistar Institute of Anatomy and Biology for his kind donation of the 452 mAb-producing hybridoma and Dr. Daniel Rodríguez for carefully reviewing the manuscript.

REFERENCES

1. Olsen, J., Kokholm, K., Noren, O., Sjostrom, H. (1997) Structure and expression of aminopeptidase N. *Adv. Exp. Med. Biol.* **421,** 47–57.
2. Look, A. T., Ashmun, R. A., Shapiro, L. H. O'Connell, P. J., Gerkis, V., d'Apice, A. J., Sagawa, K., Peiper, S. C. (1989) In *Report of the CD13 (Aminopeptidase N) Cluster Workshop, Leucocyte Typing IV* (W. Knapp, B. Doerken, W. R. Gilks, E. P. Rieber, R. E. Schmidt, H. Stein, A. E. G. K. Von dem Borne, eds.), Oxford, UK, Oxford University Press, 784.
3. Yeager, C. L., Ashmun, R. A., Williams, R. K., Gaudellicko, C. B., Shapiro, L. H., Look, A. T., Holmes, K. V. (1992) Human aminopeptidase N is a receptor for human coronavirus 229E. *Nature* **357,** 420–422.
4. Soderberg, C., Giugni, T. D., Zaia, J. A., Larsson, S., Wahlberg, J. M., Moller, E. (1993) CD13 (human aminopeptidase N) mediates human cytomegalovirus infection. *J. Virol.* **67,** 6576–6585.
5. Bhagwat, S. V., Lahdenranta, J., Giordano, R., Arap, W., Pasqualini, R., Shapiro, L. (2001) CD13/APN is activated by angiogenic signals and is essential for capillary tube formation. *Blood* **97,** 652–659.
6. Bhagwat, S. V., Petrovic, N., Okamoto, Y., Shapiro, L. (2003) The angiogenic regulator CD13/APN is a transcriptional target of Ras signaling pathways in endothelial morphogenesis. *Blood* **101,** 1818–1826.
7. Bauvois, B. (2004) Transmembrane proteases in cell growth and invasion, new contributors to angiogenesis? *Oncogene* **23,** 317–329.
8. Saiki, I., Fujii, H., Yoneda, J., Abe, F., Motowo, N., Tsuruo, T., Azuma, I. (1993) Role of aminopeptidase N (CD13) in tumor-cell invasion and extracellular matrix degradation. *Int. J. Cancer* **54,** 137–143.
9. Kido, A., Krueger, S., Haeckel, C., Roessner, A. (2003) Inhibitory effect of antisense aminopeptidase N (APN/CD13) cDNA transfection on the invasive potential of osteosarcoma cells. *Clin. Exp. Metastasis* **20,** 585–592.
10. Hoffmann, T., Faust, J., Neubert, K., Ansorge, S. (1993) Dipeptidyl peptidase IV (CD26) and aminopeptidase N (CD13) catalyzed hydrolysis of cytokines and peptides with N-terminal cytokine sequences. *FEBS Lett.* **336,** 61–64.
11. Ward, P. E., Benter, I. F., Dick, L., Wilk, S. (1990) Metabolism of vasoactive peptides by plasma and purified renal aminopeptidase. *Biochem. Pharmacol.* **40,** 1725–1732.
12. Menrad, A., Speicher, D., Wacker, J., Herlyn, M. (1993) Biochemical and functional characterization of aminopeptidase N expressed by human melanoma cells. *Cancer Res.* **53,** 1450–1455.
13. Mina-Osorio, P., Ortega, E. (2005) Aminopeptidase N (CD13) functionally interacts with FcγRs in human monocytes. *J. Leukoc. Biol.* **77,** 1008–1017.
14. Montoya, M. C., Sancho, D., Vicente-Manzanares, M., Sánchez-Madrid, F. (2002) Cell adhesion and polarity during immune interactions. *Immunol. Rev.* **186,** 68–82.
15. McIntyre, T. M., Prescott, S. M., Weyrich, A. S., Zimmerman, A. (2003) Cell-cell interactions, leukocyte-endothelial interactions. *Curr. Opin. Hematol.* **10,** 150–158.
16. Glinsky, V. V., Glinsky, G. V., Glinskii, O. V., Huxley, V. H., Turk, J. R., Mossine, V. V., Deutscher, S. L., Pienta, K. J., Quinn, T. P. (2003) Intravascular metastatic cancer cell HA at the sites of primary attachment to the endothelium. *Cancer Res.* **63,** 3805–3811.
17. Bischoff, J. (1997) Cell adhesion and angiogenesis. *J. Clin. Invest.* **99,** 373–376.
18. Cho, J. Y., Fox, D., Horejsi, V., Sagawa, K., Skubitz, K., Katz, D., Chain, B. (2001) The functional interactions between CD98, β1-integrins, and CD147 in the induction of U-937 homotypic aggregation. *Blood* **98,** 374–382.
19. Cho, J. Y., Chain, B., Vives, J., Horejsi, V., Katz, D. (2003) Regulation of CD43-induced U-937 homotypic aggregation. *Exp. Cell Res.* **290,** 155–167.
20. Kasinrerk, W., Tokrasinwit, N., Phunpae, P. (1999) CD147 monoclonal antibodies induce homotypic cell aggregation of monocytic cell line U-937 via LFA/ICAM-1 pathway. *Immunology* **96,** 184–192.
21. Campanero, M. R., Pulido, R., Ursa, A., Rodriguez-Moya, M., de Landazuri, M. O., Sanchez-Madrid, F. (1990) An alternative leukocyte homotypic adhesion mechanism, LFA-1/ICAM-l-independent, triggered through the human VLA-4 integrin. *J. Cell Biol.* **110,** 2157–2165.
22. Ikewaki, N. (1997) A novel human monoclonal antibody rapidly induces homotypic cell aggregation and promotes antibody-secreting activity by human B lymphoblastoid cell line IM-9. *J. Clin. Immunol.* **17,** 127–139.
23. Ashmun, R. A., Shapiro, L., Look, T. (1992) Deletion of the zinc-binding motif of CD13/aminopeptidase N molecules results in loss of epitopes that mediate binding of inhibitory antibodies. *Blood* **79,** 3344–3349.
24. Ashmun, R. A., Look, T. (1990) Metalloprotease activity of CD13/aminopeptidase N on the surface of human myeloid cells. *Blood* **75,** 462–469.
25. Scornik, O. A., Botbol, V. (2001) Bestatin as an experimental tool in mammals. *Curr. Drug Metab.* **2,** 67–85.
26. Santos, A. N., Langner, J., Herrmann, M., Riemann, D. (2000) Aminopeptidase N/CD13 is directly linked to signal transduction pathways in monocytes. *Cell. Immunol.* **201,** 22–32.
27. See, H., Reithmeier, R. A. (1990) Identification and characterization of the major stilbene-disulphonate-and concanavalin A-binding protein of the porcine renal brush-border membrane as aminopeptidase N. *Biochem. J.* **271,** 147–155.
28. Ishii, K., Usui, S., Sugimura, Y., Yoshida, S., Hioki, T., Tatematsu, M., Yamamoto, H., Hirano, K. (2001) Aminopeptidase N regulated by zinc in human prostate participates in tumor cell invasion. *Int. J. Cancer* **92,** 49–54.
29. Breslin, J. J., Mork, I., Smith, K., Vogel, L., Hemmila, E., Bonavia, A., Talbot, P., Sjöstrom, H., Norén, O., Holmes, K. (2003) Human coronavirus 229E, receptor binding domain and neutralization by soluble receptor at 37°C. *J. Virol.* **77,** 4435–4438.
30. Delmas, B., Gelfi, J., Kut, E., Sjöstrom, H., Norén, O., Laude, H. (1994) Determinants essential for the transmissible gastroenteritis virus-receptor interaction reside within a domain of aminopeptidase-N that is distinct from the enzymatic site. *J. Virol.* **68,** 5216–5224.
31. Xu, Y., Wellner, D., Scheinberg, D. (1997) Cryptic and regulatory epitopes in CD13/aminopeptidase N. *Exp. Hematol.* **25,** 521–529.
32. Rothlein, R., Springer, T. A. (1986) The requirement for lymphocyte function-associated antigen 1 in homotypic leukocyte adhesion stimulated by phorbol ester. *J. Exp. Med.* **163,** 1132–1149.
33. Zhou, X., Li, J., Kucik, D. F. (2001) The microtubule cytoskeleton participates in control of β2 integrin avidity. *J. Biol. Chem.* **276,** 44762–44769.
34. Woodhead, V. E., Stonehouse, T. J., Binks, M. H., Speidel, K., Fox, D. A., Gaya, A., Hardie, D., Henniker, A. J., Horejsi, V., Sagawa, K., Skubitz, K. M., Taskov, H., Todd III, R. F., van Agthoven, A., Katz, D. R., Chain, B. M. (2000) Novel molecular mechanisms of dendritic cell-induced T cell activation. *Int. Immunol.* **12,** 1051–1061.
35. Mina-Osorio, P., Ortega, E. (2004) Signal regulators in FcR-mediated activation of leukocytes? *Trends Immunol.* **25,** 529–535.
36. Delemarre, F. G., Hoogeveen, P., Haan-Meulman, M., Simons, P., Drexhage, H. (2001) Homotypic cluster formation of dendritic cells, a close

correlate of their state of maturation. Defects in the biobreeding diabetes-prone rat. *J. Leukoc. Biol.* **69,** 373–380.
37. van der Velden, V. H., Wierenga-Wolf, A. F., Adriaansen-Soeting, P. W., Overbeek, S. E., Moller, G. M., Hoogsteden, H. C., Versnel, M. A. (1998) Expression of aminopeptidase N and dipeptidyl peptidase IV in the healthy and asthmatic bronchus. *Clin. Exp. Allergy* **28,** 110–120.
38. Rosenzwajg, M., Tailleux, L., Gluckman, J. C. (2000) CD13/N-aminopeptidase is involved in the development of dendritic cells and macrophages from cord blood $CD34^+$ cells. *Blood* **95,** 453–460.
39. van der Velden, V. H., Leenen, P. J., Drexhage, H. A. (2001) CD13/aminopeptidase N involvement in dendritic cell maturation. *Leukemia* **15,** 190–191.
40. Simon, S. I., Neelamegham, S., Taylor, A., Smith, C. W. (1998) The multistep process of homotypic neutrophil aggregation: a review of the molecules and effects of hydrodynamics. *Cell Adhes. Commun.* **6,** 263–276.
41. Jacob, H. S., Hammerschmidt, D. (1981) Complement-induced granulocyte aggregation. Importance in myocardial infraction and shock lung. *JAMA* **245,** 2013–2017.